

# *Excited-state electronic asymmetry prevents photoswitching in terthiophene compounds*

Article

Accepted Version

Strudwick, B. H., Zhang, J., Hilbers, M. F., Buma, W. J., Woutersen, S., Liu, S. H. and Hartl, F. (2018) Excited-state electronic asymmetry prevents photoswitching in terthiophene compounds. *Inorganic Chemistry*, 57 (15). pp. 9039-9047. ISSN 0020-1669 doi: <https://doi.org/10.1021/acs.inorgchem.8b01005> Available at <http://centaur.reading.ac.uk/78401/>

It is advisable to refer to the publisher's version if you intend to cite from the work. See [Guidance on citing](#).

To link to this article DOI: <http://dx.doi.org/10.1021/acs.inorgchem.8b01005>

Publisher: ACS Publications

All outputs in CentAUR are protected by Intellectual Property Rights law, including copyright law. Copyright and IPR is retained by the creators or other copyright holders. Terms and conditions for use of this material are defined in the [End User Agreement](#).

[www.reading.ac.uk/centaur](http://www.reading.ac.uk/centaur)

## **CentAUR**

Central Archive at the University of Reading

Reading's research outputs online

# Excited-state electronic asymmetry prevents photo-switching in terthiophene compounds

Benjamin H. Strudwick,<sup>\*,†</sup> Jing Zhang,<sup>‡</sup> M. Hilbers,<sup>†</sup> Wybren Jan Buma,<sup>†</sup>  
Sander Woutersen,<sup>†</sup> Sheng Hua Liu,<sup>‡</sup> and František Hartl<sup>\*,¶</sup>

*Molecular Photonics Group, Van 't Hoff Institute for Molecular Sciences, University of Amsterdam, Key Laboratory of Pesticide and Chemical Biology, Ministry of Education, College of Chemistry, Central China Normal University, Wuhan 430079, P.R. China, and Department of Chemistry, University of Reading, Whiteknights, Reading RG6 6AD, United Kingdom*

E-mail: b.h.strudwick@uva.nl; f.hartl@reading.ac.uk

## Abstract

The diarylethene moiety is one of the most extensively used switches in the field of molecular electronics. Here we report on spectroscopic and quantum chemical studies of two diarylethene-based compounds with a non- $C_3$ -symmetric triethynyl terthiophene core symmetrically substituted with RuCp\*(dppe) or trimethylsilyl termini. The ethynyl linkers are strong IR markers that we use in time-resolved vibrational spectroscopic studies to get insight into the character and dynamics of the electronically excited states of these compounds on the ps-ns time scale. In combination with electronic transient absorption studies and DFT calculations our studies show that the

---

\*To whom correspondence should be addressed

<sup>†</sup>Molecular Photonics Group, Van 't Hoff Institute for Molecular Sciences, University of Amsterdam

<sup>‡</sup>Key Laboratory of Pesticide and Chemical Biology, Ministry of Education, College of Chemistry, Central China Normal University, Wuhan 430079, P.R. China

<sup>¶</sup>Department of Chemistry, University of Reading, Whiteknights, Reading RG6 6AD, United Kingdom

1  
2  
3 conjugation of the non- $C_3$ -symmetric triethynyl terthiophene system in the excited  
4 state strongly affects one of the thiophene rings involved in the ring closure. As a  
5 result, cyclisation of the otherwise photochromic 3,3''-dimethyl-2,2':3',2''-terthiophene  
6 core is inhibited. Instead, the photoexcited compounds undergo intersystem crossing  
7 to a long-lived triplet excited state from which they convert back to the ground state.  
8  
9  
10  
11  
12  
13  
14

## 15 Introduction

16  
17  
18 The top-down approach in lithography is rapidly reaching its theoretical limit, with the  
19 last decade showing solid-state devices approaching the nano-scale.<sup>1-5</sup> The bottom-up ap-  
20 proach, that is fabricating molecular devices capable of imitating macroscopic machinery,  
21 is therefore increasingly attracting attention.<sup>6-9</sup> In this bottom-up approach the reversible  
22 photoisomerization reaction of diarylethene that has been studied extensively since the first  
23 report in 1988<sup>10</sup> is an often employed component for constructing novel molecular electronic  
24 devices.<sup>11-13</sup> Diarylethene-based compounds have proven to be thermally irreversible, resis-  
25 tant to fatigue, and to exhibit a highly efficient ring closure, making them prime candidates  
26 for electronic switches.<sup>4,11,14,15</sup>  
27  
28  
29  
30  
31  
32  
33  
34  
35

36 The compounds of interest in this work, **1a** and **1b** shown in **Figure 1**, have diarylethene  
37 cores constructed using a thiophene bridging unit. The thienyl groups are attached at the 2-  
38 and 3-positions of the central bridging thiophene ring, **Figure 2**. Unlike more common bridg-  
39 ing units, such as octafluorocyclopentene, diarylmaleic anhydride or diarylmaleimide,<sup>11,16,17</sup>  
40 thiophene has the potential to reduce expenses, due to a more efficient synthesis using less  
41 volatile starting materials, which enables the upscale of production.<sup>18</sup> The terthiophene  
42 core explored in this research (**Figure 2**) has demonstrated photocyclisation,<sup>18,19</sup> thereby  
43 closely following the observation of ring closure in terthiophenes in general<sup>12</sup> with and with-  
44 out substituents on the terthiophene core.<sup>20</sup> However, it should be noted that the literature  
45 regularly reports a more commonly used diarylethene structure (1,2-bis(2-methylthiophen-  
46 3-yl)ethene) where the positions of the sulphurs differ to the ones presented here. This study  
47  
48  
49  
50  
51  
52  
53  
54  
55  
56  
57  
58  
59  
60

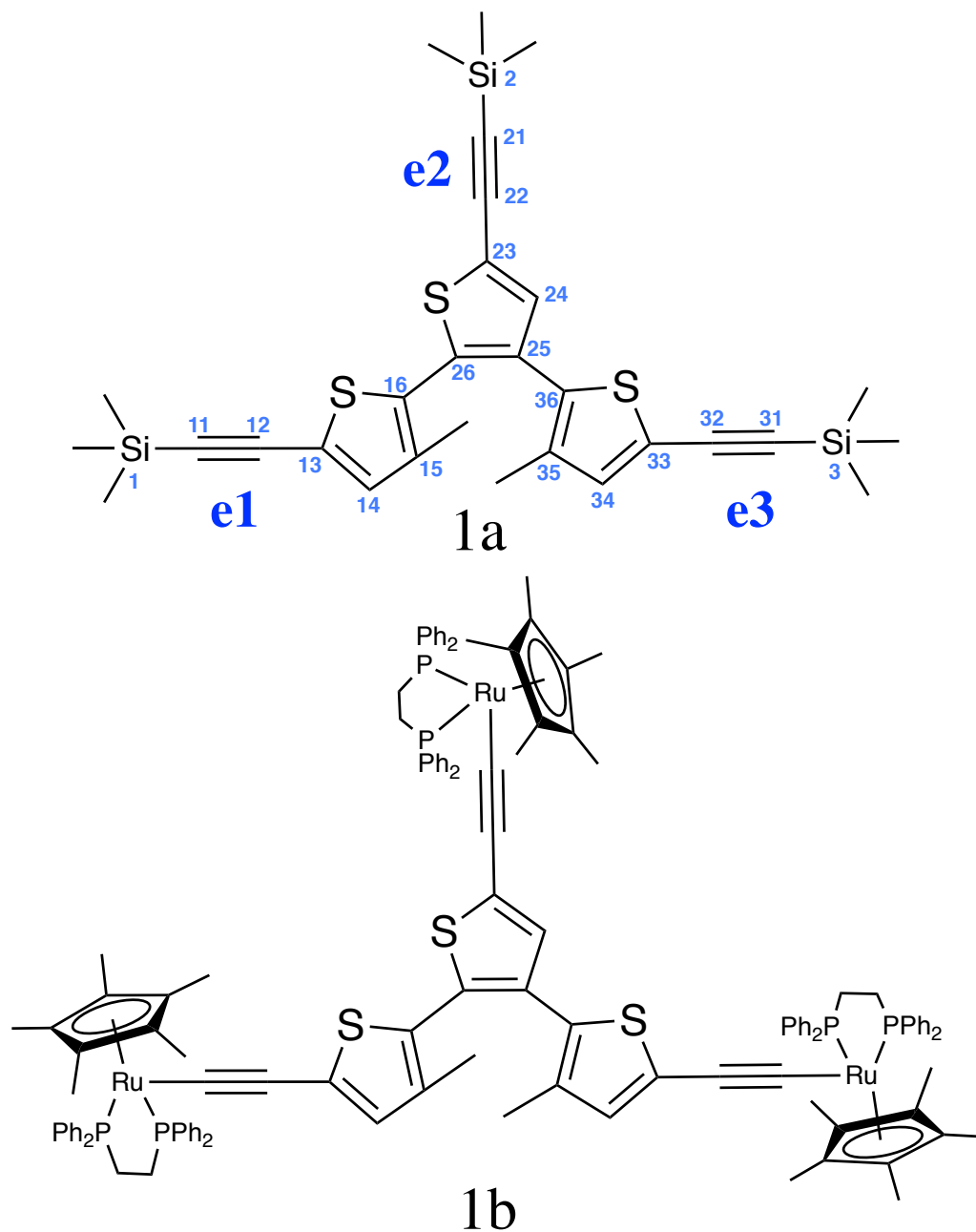


Figure 1: The studied **1a** and **1b** ethynyl-terthiophene compounds terminated with trimethylsilyl (TMS) and RuCp\*(dppe), respectively.

utilises inverse diarylethenes which have shown ring closure.<sup>21</sup> One of the main reasons for diarylethenes failing to cyclise is a result of the parallel conformation, in which the central methyl groups point in the same direction.<sup>11,22</sup> The addition of bulky groups on the other hand promote the reactive anti-parallel form.<sup>23</sup>

1  
2  
3 The motivation for investigating **1a** and **1b** is an extension of work on dinuclear organometallic-  
4 substituted diarylethenes<sup>11,17,23</sup> in which the degree of sophistication of diarylethenes was  
5 increased by creating a multifunctional (photo and redox) switch. Ethynyl-bridged metallic  
6 complexes have been extensively studied,<sup>4,24-27</sup> and found to exhibit electronic properties  
7 that are influenced by the metal and the carbon-rich bridges.<sup>26</sup> Dinuclear organometallic  
8 compounds have been constructed with central diarylethene and ethynyl-bridged metallic  
9 termini.<sup>28</sup> Importantly, these compounds retain their photochromic properties<sup>17,23</sup> but can  
10 also be switched electrochemically.<sup>16,17</sup> From this research further insight was obtained on  
11 the electronic communication between the termini in both the open and closed states.  
12  
13

14  
15  
16  
17  
18  
19  
20  
21 The alignment of a thiophene bridge to diarylethenes allowed for a terthiophene system  
22 to be investigated. The electronic and bonding properties of **1a** and **1b** have been pre-  
23 viously elucidated by anodic spectro-electrochemistry.<sup>29</sup> Compound **1a** did not show any  
24 anodic steps within the accessible potential window, nor was there any evidence for photo-  
25 cyclisation. Replacing the TMS groups in **1a** with the RuCp\*(dppe) termini in **1b** results in  
26 the appearance of three consecutive oxidation steps.<sup>29</sup> In the open form of **1b** it was found  
27 that the lateral electrophores do not communicate directly and oxidise independently. In  
28 view of previous results<sup>23</sup> that showed that the introduction of ruthenium to the system en-  
29 hances photocyclisation of diarylethene from triplet excited states, ring closure appeared to  
30 be an attractive strategy to increase the electronic communication between the electrophores.  
31 However, unlike the dinuclear analogs<sup>17,28</sup> UV/Vis spectro-electrochemistry of **1b** showed no  
32 evidence of cyclisation in any of the three anodic steps.<sup>29</sup> Since the 3,3''-dimethyl-2,2':3',2''-  
33 terthiophene core by itself does show photoreactivity,<sup>18,19</sup> it is key to understand how the  
34 highly conjugated ethynyl linkers in these systems inhibit photocyclisation, as this will pave  
35 the way for developing photoreactive trinuclear systems with a variable degree of electronic  
36 communication between the remote termini.  
37  
38  
39  
40  
41  
42  
43  
44  
45  
46  
47  
48  
49  
50  
51  
52

53 The generally accepted mechanism for cyclisation is based on the reversible electro-  
54 cyclic reaction of the central 6 $\pi$ -electron system.<sup>11,22,30,31</sup> Studies that follow these struc-  
55  
56  
57  
58  
59  
60

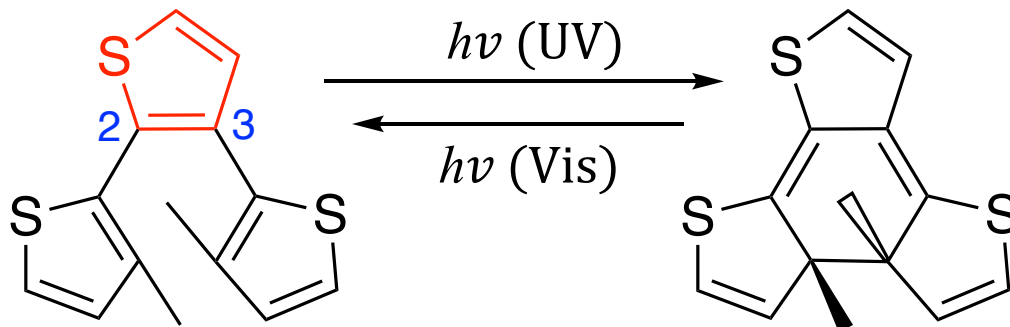


Figure 2: Photochromic reaction of non- $C_3$ -symmetric terthiophene,<sup>18</sup> constructed of diarylethenes with a thiophene-bridging unit (highlighted in red).

tural changes in real time have commonly employed UV/Vis transient absorption spectroscopy.<sup>32–37</sup> Vibrational spectroscopy has been taken advantage of by using picosecond time-resolved Stokes and anti-Stokes Raman spectroscopy<sup>38</sup> to follow the cyclisation mechanism with an experimental temporal resolution of  $\sim 4$  ps. However, femtosecond time-resolved UV/Vis-IR studies offer a significantly more detailed view on such dynamics<sup>7</sup> but as yet are absent. The ethynyl groups have demonstrated to be infrared markers that sensitively respond to changes in the oxidation state.<sup>24,29</sup> As will be shown here, time-resolved infrared spectroscopic (TR-IR) studies that target these modes are therefore an ideal means to monitor the changes that occur in the electronic structure upon excitation of the trinuclear non- $C_3$ -symmetric terthiophene compounds of interest. This, in turn, will allow us to determine the underlying reasons for the photostability of these compounds and suggest modifications to enable cyclisation.

## Experimental Methods

### Synthesis and Sample Preparation

Compounds **1a** and **1b** were synthesised as reported in the literature.<sup>29</sup> Initially, dichloromethane (DCM) dried over 4 Å molecular sieves was used as a solvent. After the discovery of photo-oxidation of **1b** in DCM (see **Section S1** in SI) anhydrous ( $\geq 99.9\%$ ), inhibitor-free tetrahy-

1  
2  
3 drofuran (THF) purchased from Sigma Aldrich was used as well as an alternative solvent. In  
4 our nanosecond UV/Vis transient absorption and time-resolved IR absorption experiments  
5 the solution was pumped through a cell so that fresh sample was probed with each laser shot.  
6 This was not possible for the femtosecond UV/Vis transient absorption experiments, but in  
7 these experiments steady-state absorption spectra taken before and after the experiments  
8 showed no degradation of **1a** in both solvents or of **1b** in THF. The sample concentrations  
9 were adjusted to obtain absorbances of 0.8 - 1 at the pump wavelength (400 nm). All samples  
10 were prepared under an inert atmosphere of dry nitrogen. The samples were bubbled with  
11 dry argon prior to the measurements. Steady-state UV/Vis and IR absorption spectra of **1a**  
12 and **1b** are given in the SI, **Section S2**.  
13  
14  
15  
16  
17  
18  
19  
20  
21  
22  
23

## 24 Femtosecond Transient Spectroscopy

25  
26  
27 Time-resolved infrared spectroscopy was performed using commercially available Ti:sapphire  
28 lasers (Spectra-Physics Hurricane, 600  $\mu\text{J}$ ,  $\sim 100$  fs FWHM and Coherent, 2 mJ,  $\sim 50$   
29 fs FWHM). With the amplified output from these lasers and an optical setup described  
30 elsewhere,<sup>39</sup> mid-IR pulses with a duration of 200 fs, a bandwidth of 150  $\text{cm}^{-1}$  and an  
31 energy of 1 - 3  $\mu\text{J}$  were produced. UV-pump pulses at 400 nm with energies of 4  $\mu\text{J}$  were  
32 generated by doubling the amplified 800 nm output with a type II BBO crystal, and were  
33 delayed by mechanically adjusting the beam path. The UV pump was focused and spatially  
34 overlapped with the mid-IR probe, and a temporal resolution of  $\sim 200$  fs (FWHM) was  
35 determined as described previously.<sup>7</sup> The signals were recorded using an electronically gated  
36 amplifier, an Oriel M260i spectrometer and a 32 pixel MCT detector. The samples, in a  
37 flow cell equipped with  $\text{CaF}_2$  windows spaced by 1 mm, were placed in the mid-IR focus and  
38 pumped through the cell to ensure a fresh sample being measured with each laser shot.  
39  
40  
41  
42  
43  
44  
45  
46  
47  
48  
49  
50

51 Femtosecond visible transient absorption experiments were performed with the Spectra-  
52 Physics Hurricane system mentioned above. 2.5% of the 800 nm fundamental light was  
53 used to generate a white-light continuum from 350 to 850 nm by focusing on a  $\text{CaF}_2$  plate.  
54  
55  
56  
57  
58  
59  
60



1  
2  
3 The fundamental light used for the white-light generation was passed twice over a delay  
4 stage, providing up to 3.6 ns time delay. The sample cell was a 1 mm quartz cuvette. The  
5 pump light (400 nm) was created as mentioned above and ran at 500 Hz, using a mechanical  
6 chopper to produce a non-pumped signal acting as a reference measurement. The spectra  
7 were measured using a spectrograph (Shamrock 193i with a 150 lines/mm grating) and a  
8 single diode-array (Hamamatsu NMOS S3901-512Q) detector. The readout was done using  
9 fast electronics (TEC5).  
10  
11  
12  
13  
14  
15  
16  
17  
18

## 19 Nanosecond Transient Spectroscopy

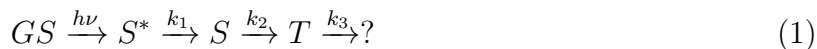
20  
21 Nanosecond transient absorption was measured using an in-house assembled setup described  
22 elsewhere.<sup>40</sup> A tunable Nd:YAG-laser system (NT342B, Ekspla) produced the 400-nm pump  
23 pulse of 1 mJ that passed through the sample orthogonal to the probe light. The white-light  
24 source was a high-stability short-arc xenon flash lamp (FX-1160, Excelitas Technologies)  
25 with a modified PS302 controller (EG&G). Transient absorption spectra were measured on  
26 a gated intensified CCD camera (PI-MAX3, Princeton Instruments) using a 10 ns gate. The  
27 samples were continuously pumped through a 1 cm quartz cuvette, so that only fresh samples  
28 were measured.  
29  
30  
31  
32  
33  
34  
35  
36  
37  
38

## 39 DFT and TD-DFT Calculations

40  
41 (TD-)DFT calculations have been performed with the Gaussian09 software package.<sup>41</sup> **1a**  
42 geometry optimisation, electronic vertical transitions and frequency calculations were per-  
43 formed at the B3LYP/6-31G(d) level of theory chosen for its good performance with this  
44 type of molecular systems.<sup>42-45</sup> Solvent effects (DCM) were included using the Polarizable  
45 Continuum Model.<sup>46</sup> **1b** (TD-)DFT calculations have been performed in vacuum at the  
46 CAM-B3LYP/LANL2DZ level of theory.<sup>47,48</sup>  
47  
48  
49  
50  
51  
52  
53  
54  
55  
56  
57  
58  
59  
60

## Results and Discussion

To obtain insight into the optically excited state of **1a** and its dynamics, we first performed femto- and nanosecond vis-pump/vis-probe experiments in THF (**Figures 3** and **4**, respectively). Femto- and nanosecond transient spectra were also recorded in DCM (SI, **Section S3** (**Figures S7** and **S8**)), with no appreciable difference as compared to THF. In both solvents, **1a** was optically excited with 400 nm photons. TD-DFT calculations of the vertical transitions from the ground state show that the transition with the lowest excitation energy occurs at 3.11 eV (398 nm) with an oscillator strength of  $f=0.7217$ , and that it is predominantly described by the HOMO  $\rightarrow$  LUMO (SI, **Section S4** (**Figure S10**)) excitation. The calculated electronic absorption spectrum (SI, **Section S4** (**Figure S13**)) is in good agreement with steady-state UV-Vis spectra of **1a**, (SI, **Section S2** (**Figure S5**)). In the transient spectra (**Figure 3**) of **1a** we can distinguish three spectral features. Initially, within a few ps, a broad feature is seen across the entire spectral window with two distinctive maxima at 550 and 705 nm. From this state it converts to a second state that is blue-shifted by ca. 25 nm (evident from the decay-associated spectra (DAS) shown in the SI, **Section S3** (**Figure S9**)) but maintains similar spectral features, hinting the initial state to be a hot singlet-excited state. Subsequently a third feature showing a strong absorption at roughly 400 - 550 nm becomes apparent. This third transient species does not decay within the 4 ns delay range accessible in our femtosecond setup. The transient data matrix for the femtosecond time domain was globally fitted using an open-source program Gloteran,<sup>49</sup> assuming a sum of exponential time profiles and a sequential model (1):



In this model vertical excitation ( $h\nu$ ) populates a hot singlet state  $S^*$  which is converted into a relaxed singlet state  $S$  with a time constant of  $\tau_1 = 7 \pm 2$  ps. The transition from the relaxed singlet state to the triplet state  $T$  (as follows from the TR-IR data and TD-DFT

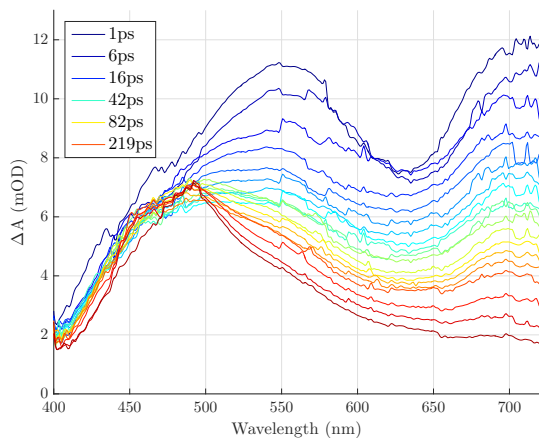


Figure 3: Femtosecond UV/Vis transient absorption spectra of **1a** in THF excited at 400 nm. The DAS is shown in the SI, **Figure S9**.

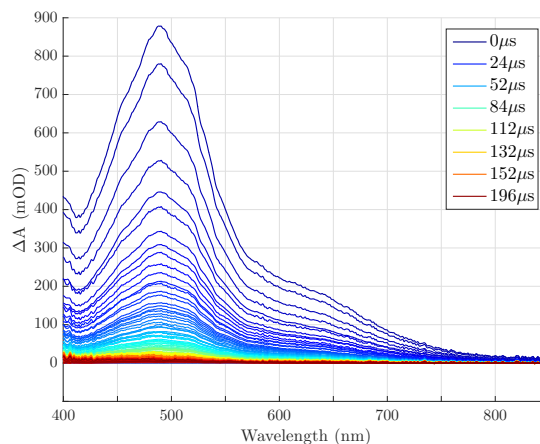


Figure 4: Nanosecond UV/Vis transient absorption spectra of **1a** in THF excited at 400 nm.

calculations discussed below) takes  $\tau_2 = 119 \pm 2$  ps. The DAS, from the electronic differential absorption measurements, of the  $S^*$ ,  $S$  and  $T$  states of **1a** are given in the SI (**Section S3** (**Figure S9**)). In order to further monitor the decay of these electronically excited molecules, nanosecond transient absorption spectra were recorded for **1a** (**Figure 4**) excited at 400 nm. Singular Value Decomposition (SVD)<sup>50</sup> of the nanosecond transient spectra shows the decay of a single transient species. We have therefore, using model (2), performed a global analysis of the nanosecond transient data matrix assuming a sum of exponential time profiles and T-T annihilation (described in detail in **Section S5** in the SI):



From these fits we find a lifetime of the triplet state of  $\tau_3 = 22.7 \pm 0.5 \mu s$ , fits are shown in **Figure 5**. The spectral features in the visible region in the nanosecond time domain show no evidence of other transient species, and the long lifetime provides further evidence for triplet-state formation. For aerated solutions the rate of the  $T \rightarrow GS$  conversion increased for **1a** ( $\tau_{3,air} = 410 \pm 2$  ns), again confirming that  $T$  is a triplet state.

Complementary TR-IR experiments were performed to obtain a better insight into the

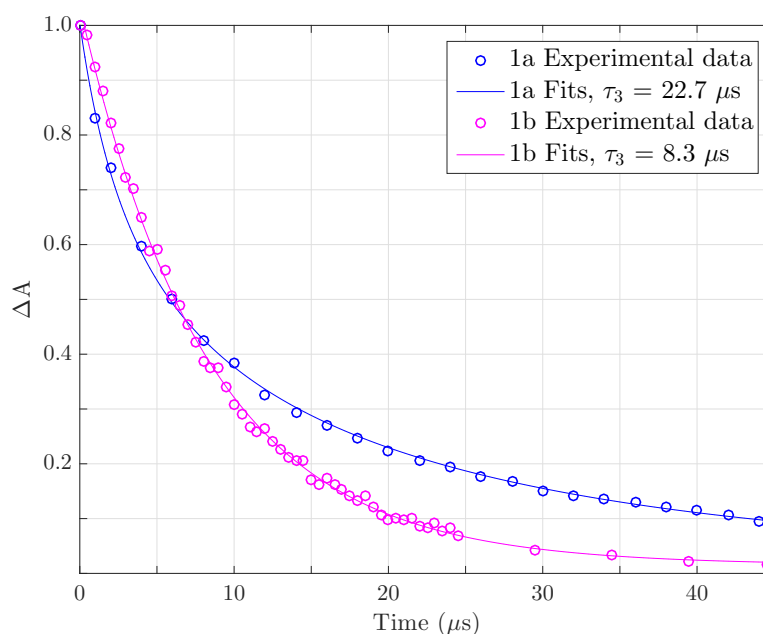


Figure 5: Decay of the transient absorption signal of **1a** (**1b**) at 580 (650) nm in the nanosecond time domain. Spectral absorbances have been normalised.

electronic structure of each excited state and to determine what inhibits photocyclisation of **1a**. The evolution of the TR-IR spectra of **1a** after excitation at 400 nm is shown in **Figure 6**. Adopting a target model (1), global fits of the TR-IR spectra lead to time constants of  $\tau_1 = 3.0 \pm 1$  ps and  $\tau_2 = 114 \pm 2$  ps for **1a**, and the TR-IR decay-associated spectra (TR-IR DAS) that are shown in (**Figure 6**). Comparison of the TR-IR DAS of the initial species ( $S^*$ ) with that of the second species (S) reveals a narrowing of the induced absorption band and shift to a slightly higher energy of  $\sim 3 \text{ cm}^{-1}$ , in line with the conclusion that vibrational cooling of the hot excited singlet state occurs. The femtosecond TR-IR measurements thus confirm that the initial  $S^*$  state is a hot electronically excited state (note that the TA and TR-IR transients have the same rates of decay). Importantly, neither type of experiments indicates the presence of a ring-closed species. Various parameters such as solvent polarity and excitation wavelength have been changed to see whether under different conditions cyclisation might occur, but in all cases no indication was found for cyclisation or even a markedly different transient behaviour.

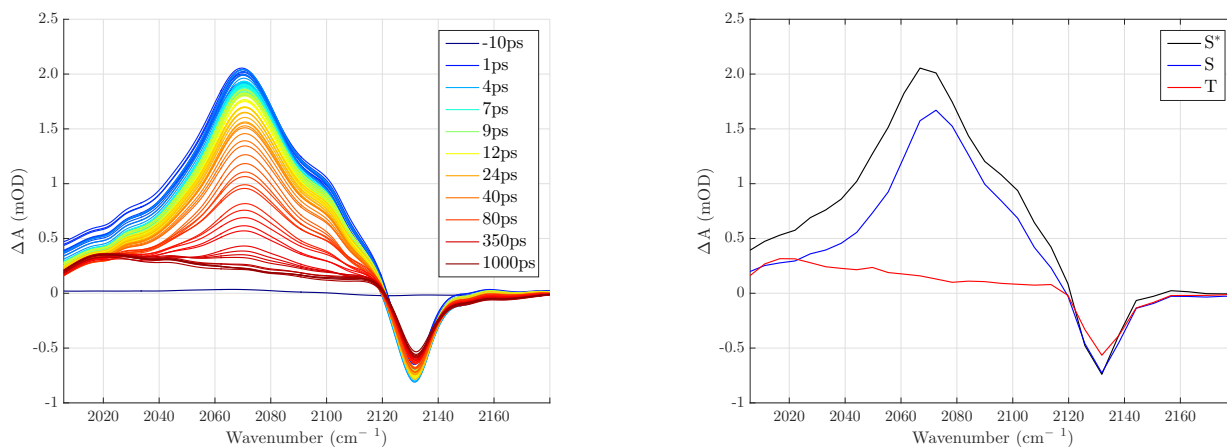


Figure 6: Left: Femtosecond TR-IR spectra of **1a** in DCM and excited at 400 nm. Right: TR-IR decay-associated spectra (DAS) derived from the TR-IR spectra of **1a**.

**Figure 7** shows DFT and TD-DFT predicted IR absorption spectra in the ethynyl stretching region for the ground and excited states of **1a**, with frequencies scaled by 0.95 (which closely follows what is reported in the literature<sup>51</sup>) and presented in **Table 1**. Overall good agreement is observed between the experimental and theoretical spectra. Experimentally a ground-state (GS) bleach is observed at  $2135\text{ cm}^{-1}$ . The calculations show that this band actually consists of three unresolved bands from the three different stretching modes of the ethynyl linkers. The calculated highest-frequency mode at  $2136\text{ cm}^{-1}$  involves mainly the central thiophene ethynyl, labelled **e2** in **Figure 1**. The lower-frequency components at  $2132\text{ cm}^{-1}$  and  $2131\text{ cm}^{-1}$  are assigned to the symmetric and antisymmetric stretching modes of the ethynyl linkers at the lateral thiophenes (**e1** and **e3** in **Figure 1**). From the experimentally observed and theoretically predicted small frequency differences one can thus conclude that in the ground state all three linkers are more or less equivalent, and that a complete delocalisation of the vibrational excitation occurs over the terthiophene backbone.

This is in marked contrast with the initial singlet excited state (S in **Figures 6** and **7**), for which there is a lowering of energy of the bands. This is observed in both the experimental and theoretical spectra. The lower energy indicates a weakening of the ethynyl bonds and is in line with what one would expect, but much more surprising is the observation that there

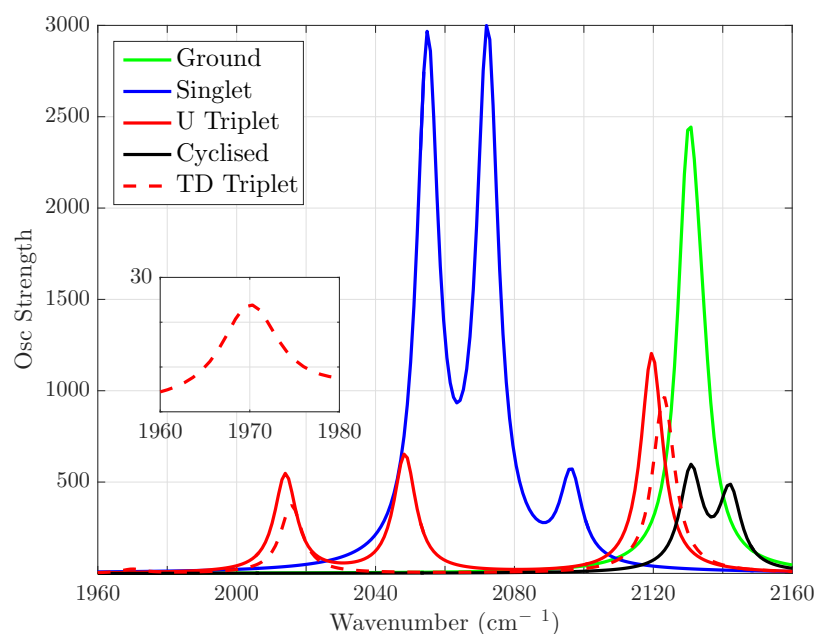


Figure 7: Theoretically predicted IR absorption spectra of the ground state, the lowest excited singlet state and the lowest excited triplet state of the open form of **1a** as well as of the ground state of its cyclised form. All calculated modes have been broadened to give a FWHM of  $4\text{ cm}^{-1}$ .

are three very distinct bands, since this can only be explained by assuming that the electronic excitation is not equally delocalised over the three linkers. Our calculations show that the main contributions to the experimentally observed absorption bands at 2097, 2075 and 2069  $\text{cm}^{-1}$  come from **e3**, **e2** and **e1**, respectively (**Figure 1**). These frequency differences nicely follow the changes in bonding character that arise from the HOMO  $\rightarrow$  LUMO transition (SI, **Section S4 (Figure S10)**), which takes the **e1** C $\equiv$ C from a bonding state in the HOMO to an antibonding state in the the LUMO. For the **e2** C $\equiv$ C the antibonding character is less pronounced than for **e1**, and even less for the **e3** C $\equiv$ C for which the LUMO is almost non-bonding. The asymmetry of the non- $C_3$ -symmetric terthiophene core thus has dramatic consequences for the character of the excitation, for which we can now conclude is strongly localised on the **e1** thiophene arm, to a lesser extent on the **e2** arm, and leaves the **e3** arm practically unaffected.

TD-DFT calculations have also been performed for the lowest excited triplet state (**Figure**

7). The agreement between theory and experiment is in this case considerably less than observed above for the lowest excited singlet state. Interestingly, we find that calculations at the unrestricted DFT (U-DFT) level lead to a much better agreement (see **Figure 7**) indicating that a variational treatment apparently is better able to recover the character of this state than the perturbation approach used in TD-DFT (this has been found to be the case for similar systems in the literature<sup>52-54</sup>). Inspection of the modes calculated at the U-DFT level shows that the mode calculated at 2014  $\text{cm}^{-1}$  is associated with the asymmetric stretching mode of **e1** and **e2** with the major contribution coming from **e1**. The corresponding symmetric stretching mode with **e2** being most involved is found at 2048  $\text{cm}^{-1}$ , while the **e3** stretching is solely responsible for the IR absorption at 2119  $\text{cm}^{-1}$ . The latter mode is not directly apparent in the experimental TRIR spectra because of its overlap with the GS bleach, but on closer inspection can be found by the shoulder that is visible at about 2110  $\text{cm}^{-1}$  and the partial recovery of the GS bleach at a similar rate as the population of the triplet state.

Previously we have concluded that in the lowest excited singlet state the excitation is strongly localised on two of the arms. Comparison of the IR absorption spectra of the lowest excited singlet and triplet states shows that in the lowest triplet state such a localisation is even more pronounced. The frequency of the **e3**  $\text{C}\equiv\text{C}$  stretch mode increases with energy with respect to that of the lowest excited singlet state and almost the same as in the ground state while at the same time the absorption bands associated with the **e1** and **e2**  $\text{C}\equiv\text{C}$  stretch modes undergo a decrease in energy.

**Figure 7** and **Table 1** also present DFT-calculated IR absorption bands for the ground state of the hypothetical photo-cyclised form of **1a**. Here we find symmetric and antisymmetric combinations of **e1** and **e3** at 2141 and 2142  $\text{cm}^{-1}$ , respectively, while the stretch mode of the central **e2** ethynyl group is calculated at 2129  $\text{cm}^{-1}$ . Despite the lack of experimental evidence for photo-cyclisation, the DFT calculations do not exclude its occurrence. Relative to the GS the S is 61.3  $\text{kcal mol}^{-1}$  higher in energy. The T(U) is calculated to

be 42.8 kcal mol<sup>-1</sup> higher than the GS while the T(TD) predicts it to be 36.5 kcal mol<sup>-1</sup> higher than the GS. The energy of **1a** is about 35 kcal mol<sup>-1</sup> higher for the cyclised complex compared to the parent open-triangle form in the GS. Hence, cyclisation from the S state or the triplet state (either the U or TD) is energetically feasible; albeit the TD calculated triplet state energy is very close to that of the cyclised compound. Therefore it is likely there is a high activation barrier in all the excited states that cannot be overcome.

Table 1: Calculated frequencies of **1a** (scaled by 0.95) and experimentally observed frequencies of **1a** and **1b**.

Bond	Calculated Frequencies of <b>1a</b> (cm <sup>-1</sup> )				
	GS	S	T(TD)	T(U)	Cyclised
<b>e1</b>	2132	2054	1969	2014	2141
<b>e2</b>	2136	2074	2015	2048	2129
<b>e3</b>	2131	2095	2122	2119	2142
Compound	Measured Frequencies of <b>1a</b> and <b>1b</b> (cm <sup>-1</sup> )				
	GS	S	T	Oxidised	
<b>e1 (1a)</b>	2135	2069	2019	-	
<b>e2 (1a)</b>	-	2075	2050	-	
<b>e3 (1a)</b>	-	2097	2118	-	
<b>e1 (1b)</b>	2050	1936	1936	1935 <sup>29</sup>	
<b>e2 (1b)</b>	-	1980	1980	1992 <sup>29</sup>	
<b>e3 (1b)</b>	-	2020	2030	2049 <sup>29</sup>	

Another possible reason that photoexcitation does not lead to cyclisation could be that the methyl groups do not have the appropriate orientation for ring closure to occur. Previous work<sup>11,13</sup> has shown that for the parallel conformer cyclisation is inhibited. Although DFT calculations do not show an appreciable energy difference between the two forms, the anti-parallel form being a mere 0.1 kcal mol<sup>-1</sup> lower in energy, NOESY measurements on **1a** (SI, **Section S6 (Figures S15 and S16)**) provide no evidence for the presence of the parallel conformer in the ground state. Upon excitation the anti-parallel form might convert to the parallel conformer by rotation about one of the bridging bonds, viz.  $C_{16} - C_{26}$  or  $C_{25} - C_{36}$



1  
2  
3 (Figure 1). SVD<sup>50</sup> in the nanosecond time domain reveals only a single transient species,  
4 while the picosecond dynamics can be well explained by vibrational cooling and intersystem  
5 crossing to the triplet manifold. The literature, backed up by our NMR measurements (SI,  
6 Section S6 (Figure S17)), also rules out *E/Z*-isomerization as a possible reason for absence  
7 of cyclisation, as the bridging thiophene unit prevents the formation of the *E*-form.<sup>13</sup>  
8  
9

10  
11 The TR-IR measurements backed up by the TD-DFT calculations show that the HOMO  
12 has equal contributions from the three arms but that the LUMO resides heavily on the  
13 left side of **1a**. These orbitals closely resemble the analogous orbitals found in previous  
14 work<sup>29</sup> on **1b**. In line with our conclusions regarding the influence of the asymmetry on the  
15 electronic properties, calculations on **1b**<sup>+</sup> show that in the oxidised form the spin density  
16 asymmetrically distributed with the largest contributions from the thiophenes involved in  
17 the **e1** and **e2** arms. The asymmetry by itself cannot be the only reason why **1a** does  
18 not undergo ring closure, since from previous studies it is known that non-*C*<sub>3</sub>-symmetric  
19 terthiophene cores<sup>18,19</sup> can cyclise. In the following we will argue that the attachment of the  
20 ethynyl-based substituents onto the non-*C*<sub>3</sub>-symmetric terthiophene core lead to changes in  
21 the conjugation which in turn are expected to have a major impact on the photocyclisation  
22 pathway.  
23  
24  
25  
26  
27  
28  
29  
30  
31  
32  
33  
34  
35  
36

37 Our TR-IR studies show that electronic excitation has a large influence on the bonding  
38 properties of the **e1** ethynyl linker: instead of the triple bond character it has in the ground  
39 state, bonding becomes reduced. The same is true for the **e2** ethynyl linker albeit to a  
40 lesser extent. In terms of valence bond structures this implies that the contribution of the  
41 structure depicted in **Figure 8** to the electronic wavefunction is increased considerably in the  
42 electronically excited states. Our observation that in the photoexcited triplet state bonding  
43 characters are more reduced than in the photoexcited singlet state demonstrates that in the  
44 triplet state this mesomeric structure has an even larger contribution than in the singlet  
45 state. This increased contribution has a major impact on the conjugation in both states as  
46 becomes clear from the bond lengths reported in the **Table S1, Section S4** of the SI. The  
47  
48  
49  
50  
51  
52  
53  
54  
55  
56  
57  
58  
59  
60

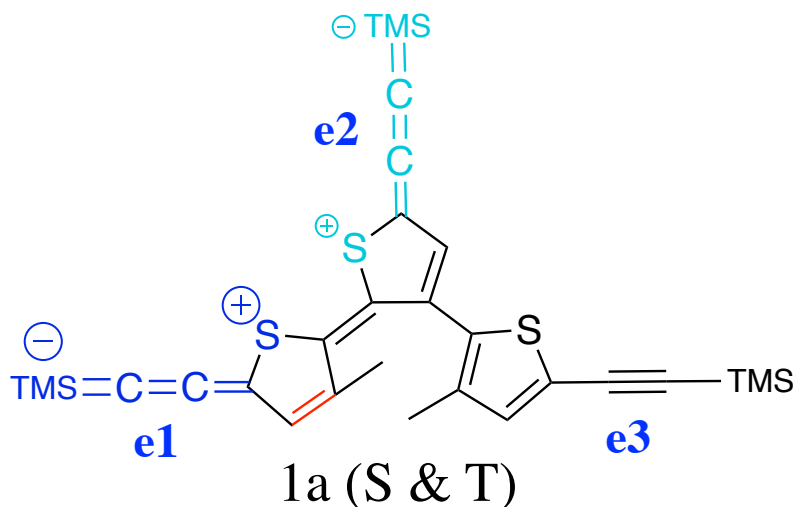


Figure 8: Valence bond structure of **1a** that gains importance in the singlet and triplet excited states. Charge size and colour annotated on the arms indicate the degree of charge separation, the **e1** arm thus having a larger degree of charge separation than **e2**.

calculations show that the **e1** and **e2** ethynyl bonds  $C_{11} - C_{12}$  and  $C_{21} - C_{22}$  (numbered in **Figure 1**) lengthen in both S and T compared to GS while for the **e3** ethynyl bond  $C_{31} - C_{32}$  the change in bond length is much smaller. At the same time, they show for the thiophene ring attached to **e1** a sizable shortening of the  $C_{14} - C_{15}$  bond (a change in the electron density of this bond, from the HOMO to the LUMO, can be clearly seen in the SI **Section S4 (Figure S11)**) and a lengthening of  $C_{13} - C_{14}$  and  $C_{15} - C_{16}$  bonds, giving rise to a quasi inversion of single and double bond character upon excitation. Finally, also the  $C_{16} - C_{26}$  bond connecting the **e1** and **e2** thiophene arms changes from a single into a double bond. Analogous but smaller changes are observed for the **e2** arm while the **e3** arm is hardly affected. Cyclisation is clearly a highly unfavourable process for the mesomeric structure depicted in **Figure 8**. In order to cyclise the  $C_{13} - C_{14}$  bond, which has been shown to have double bond like characteristics in the excited state (SI, **Section S4 (Figure S11)**), would have to become unsaturated, having a knock on effect on the conjugation throughout the whole molecule. The increased contribution in the electronically excited states thus provides a logical explanation for the absence of photocyclisation in both the singlet and triplet states.

The insight that we have now acquired on the electronic structure of **1a** and how this

1  
2  
3 structure changes upon photoexcitation provides an excellent starting point for assessing  
4 the influence of the ruthenium termini in **1b**. Importantly, **1b** also enables us to compare  
5 the properties of the photo-excited compound with those of the electrochemically oxidised  
6 one which was not possible for **1a** as electrochemical studies of the latter have not been  
7 reported yet. **Figure 9** displays nanosecond UV/Vis transient absorption spectra of **1b**.  
8 Nanosecond UV/Vis transient absorption experiments show that photoexcitation of **1b** in  
9 THF eventually populates the triplet state T (**Figure 9**). As a result of the ruthenium  
10 termini absorption from T now occurs at ca. 650 nm and is thus strongly red-shifted from  
11 the ca. 480 nm absorption observed for **1a**. Global analysis of these data using model S1 (SI,  
12 **Section S5**) that assumes a sum of exponential time profiles and triplet-triplet annihilation  
13 lead to a time constant  $\tau_3 = 8.3 \pm 0.5 \mu\text{s}$  for the T  $\rightarrow$  GS decay which is a factor three faster  
14 than observed for **1a**, fits are shown in **Figure 5**. This increase in decay rate is not surprising  
15 in view of the increased spin-orbit coupling in **1b** due to the Ru atoms. Femtosecond UV/Vis  
16 transient absorption spectra of **1b** (SI, **Section S7 (Figure S18)**) show that the triplet  
17 state is populated within the first 20 ps but do not provide a clear view on the early-time  
18 dynamics.

19  
20  
21  
22  
23  
24  
25  
26  
27  
28  
29  
30  
31  
32  
33  
34  
35  
36  
37  
38  
39  
40  
41  
42  
43  
44  
45  
46  
47  
48  
49  
50  
51  
52  
53  
54  
55  
56  
57  
58  
59  
60  
Previously, it has been shown that attachment of the ethynyl-metal based substituents  
onto a symmetric terthiophene core does not impede cyclisation.<sup>17,23</sup> In the present exper-  
iments, in contrast, we do not observe any evidence for cyclisation. In fact, from the full  
recovery of the GS bleach in **Figure 9** it can be concluded that in THF **1b** completely  
reverts back to the GS.

TR-IR spectra of **1b** are shown in **Figure 10**. Global analysis of these spectra gives  
rise to two species with DAS that are displayed in **Figure 10**. The final species can clearly  
be associated with T which is populated with a time constant of  $\tau_2 = 5 \pm 2$  ps. This is  
considerably faster than what is observed for **1a** but entirely in line with the strong spin-  
orbit coupling due to the presence of the Ru atoms that was previously concluded to be  
responsible for the increased decay rate of the triplet to the ground state. The assignment

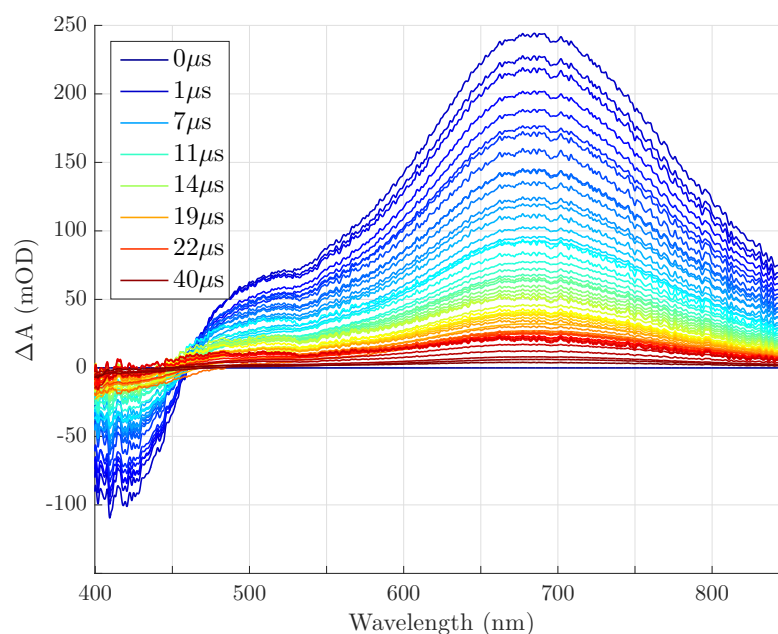


Figure 9: Nanosecond UV/Vis transient absorption spectra of **1b** in THF excited at 400 nm.

of the first species, on the other hand, is not directly clear. It could be associated with the initially excited singlet state, but this would imply that the excited singlet and triplet states have very similar ethynyl stretch frequencies which—in view of our observations for **1a** where distinct IR absorption spectra were observed for both states—would not directly be expected. Alternatively, the narrowing of the bands in the DAS of the second species as compared to those in the first species and the decay rate of the first species would be in line with a vibrational cooling process occurring in the triplet manifold. In that case intersystem crossing would be faster than the  $\sim 1$  ps time resolution of our TR-IR experiments.

Comparison of the ethynyl vibrational characteristics of **1a** and **1b** shows that in the ground state of **1b** frequencies are reduced by about  $100\text{ cm}^{-1}$ , indicating delocalisation of the conjugation over the Ru termini, this is backed up by the HOMO plots of **1b** in the SI **Section 4 (Figure S12)**. However, in the triplet state the ethynyl modes undergo the same asymmetric frequency shifts in **1b** as in **1a** as can be concluded from **Table 1**. We thus conclude that in both compounds electronic excitation leads to very similar changes in the

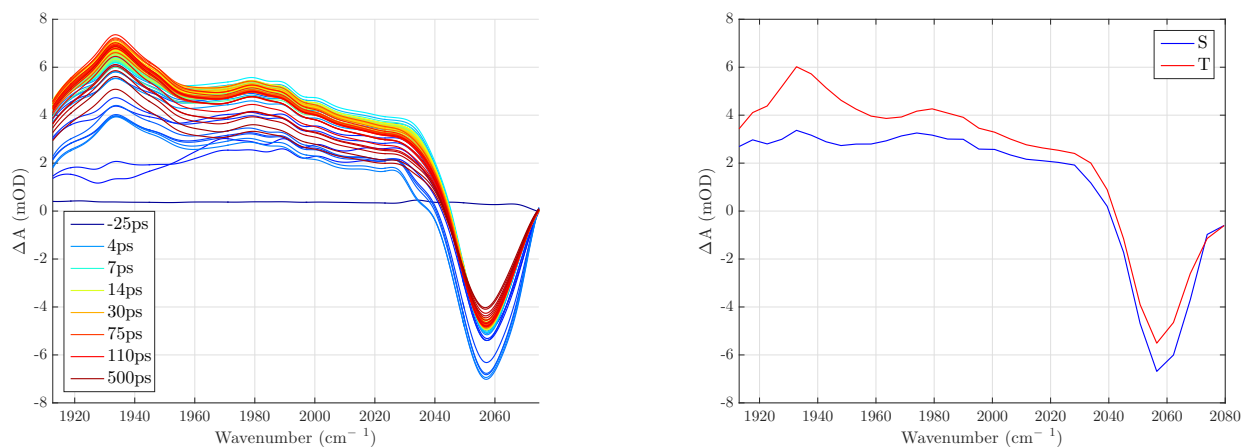


Figure 10: Left: Femtosecond TR-IR spectra of **1b** in THF excited at 400 nm. Right: TR-IR decay-associated spectra (DAS) of **1b**.

electronic structure, and in particular to an increase of the contribution of the mesomeric structure shown in **Figure 8**. In **Section S4 (Figure S12)** of the SI the LUMO + 1 of **1b** is shown. The calculations of the 10 lowest energy vertical transitions are shown in the SI **Section S4 (Figure S14)** which show one dominant transition associated with the HOMO  $\rightarrow$  LUMO + 1 transition. The comparison of the LUMO of **1a** and the LUMO + 1 of **1b** confirms the similarities between the excited states, especially when comparing the LUMO/LUMO + 1 on the  $C_{14} - C_{15}$  bond of the two compounds. It would therefore appear that modifying the arms with the Ru termini —aiming thereby to change the asymmetry in the character of the electronically excited states as well— does not change the conjugation to such an extent that cyclisation becomes possible.

Interestingly, we find that the changes in the ethynyl frequencies in the triplet state of **1b** closely follow the changes when **1b** is oxidised (**Table 1**).<sup>29</sup> The asymmetry in the electronic wavefunction of **1b<sup>+</sup>** is further supported by the spin density distribution which is found to reside heavily on the lateral side of **1b<sup>+</sup>** between **e1** and **e2**. Moreover, the electronic absorption spectrum from the triplet state of **1b** and the ground state of **1b<sup>+</sup>** show similar features, both having strong absorption bands with maxima at ca. 730 nm for **1b<sup>+</sup>** (SI, **Section S1 (Figure S3)**) and ca. 680 nm for the T state (**Figure 9**). These

1  
2  
3 spectroscopic markers thus indicate that **1b** in its lowest excited triplet state is similar to  
4 the ground state of the one-electron oxidised form. This suggests that the photoinduced  
5 promotion of an electron from the HOMO to the antibonding LUMO (**1a**)/ LUMO + 1 (**1b**)  
6 and the complete electrochemical removal of an electron from the HOMO both result in a  
7 similar weakening of the **e1** and **e2** ethynyl characteristics and modified conjugation in the  
8 terthiophene core.  
9  
10  
11  
12  
13  
14  
15  
16

## 17 Conclusions

18  
19  
20 To summarise, we have investigated two open-triangle triethynyl terthiophene compounds,  
21 **1a** and **1b**, that show a surprising photostability instead of switchable photocyclisation.  
22 Visible transient spectroscopy has unveiled the decay pathways of both compounds that  
23 populate the triplet state manifold. Using the ethynyl groups as sensitive IR markers for  
24 the electronic structure of these compounds in ground and electronically excited states, we  
25 have shown that in both compounds electronic excitation induces an electronic asymmetry  
26 in the terthiophene core. The concurrent reduction of electronic delocalization has far-  
27 reaching consequences, as it increases the importance of mesomeric structures that do not  
28 favor cyclization —as is indeed observed. Although the addition of the Ru termini extends  
29 delocalization of the electronic wavefunction in the ground state, it does not modify the  
30 electronic structure of the electronically excited states as to enable cyclization.  
31  
32  
33  
34  
35  
36  
37  
38  
39  
40  
41  
42

43 The present study has revealed what prevents photocyclization in these asymmetric ter-  
44 thiophene compounds. It thereby provides a solid starting point for designing novel com-  
45 pounds in which asymmetry could be compatible with gating electron and energy transfer  
46 using photocyclization and electrochemistry. Such studies are presently underway.  
47  
48  
49  
50  
51  
52  
53  
54  
55  
56  
57  
58  
59  
60

## Acknowledgement

The author SW kindly acknowledges the John van Geuns foundation for financial support. The authors JZ, SHL and FH gratefully acknowledge financial support from the National Natural Science Foundation of China (21472059), the Overseas Talent Plan 111 Project B17019. This work was supported by the Nederlandse Organisatie voor Wetenschappelijk Onderzoek (NWO).

## References

- (1) Carroll, R. L.; Gorman, C. B. The Genesis of Molecular Electronics. *Angew. Chem. Int. Ed.* **2002**, *41*, 4378–4400.
- (2) Joachim, C.; Gimzewski, J. K.; Aviram, A. Electronics using hybrid-molecular and mono-molecular devices. *Nature* **2000**, *408*, 541–548.
- (3) Low, P. J. Metal complexes in molecular electronics: progress and possibilities. *Dalton Trans.* **2005**, 2821–2824.
- (4) Xiang, D.; Wang, X.; Jia, C.; Lee, T.; Guo, X. Molecular-Scale Electronics: From Concept to Function. *Chemical Reviews* **2016**, *116*, 4318–4440.
- (5) Lörtscher, E. Wiring molecules into circuits. *Nature Nanotechnology* **2013**, *8*, 381–384.
- (6) Panman, M. R.; Bodis, P.; Shaw, D. J.; Bakker, B. H.; Newton, A. C.; Kay, E. R.; Brouwer, A. M.; Buma, W. J.; Leigh, D. A.; Woutersen, S. Operation Mechanism of a Molecular Machine Revealed Using Time- Resolved Vibrational Spectroscopy. *Science* **2010**, *328*, 1255–1258.
- (7) Panman, M. R.; Bodis, P.; Shaw, D. J.; Bakker, B. H.; Newton, A. C.; Kay, E. R.; Leigh, D. A.; Buma, W. J.; Brouwer, A. M.; Woutersen, S. Time-resolved vibrational spectroscopy of a molecular shuttle. *Phys. Chem. Chem. Phys.* **2012**, *14*, 1865–1875.

- 1  
2  
3 (8) Bissell, R. A.; Córdova, E.; Kaifer, A. E.; Stoddart, J. F. A chemically and electro-  
4 chemically switchable molecular shuttle. *Nature* **1994**, *369*, 133–136.  
5  
6  
7  
8 (9) Brouwer, A. M.; Frochot, C.; Gatti, F. G.; Leigh, D. A.; Mottier, L.; Paolucci, F.;  
9 Roffia, S.; Wurpel, G. W. H. Photoinduction of Fast, Reversible Translational Motion  
10 in a Hydrogen-Bonded Molecular Shuttle. *Science* **2001**, *291*, 2124–2128.  
11  
12  
13  
14 (10) Nakamura, S.; Irie, M. Thermally irreversible photochromic systems. A theoretical  
15 study. *J. Org. Chem.* **1988**, *53*, 6136–6138.  
16  
17  
18  
19 (11) Irie, M.; Fukaminato, T.; Matsuda, K.; Kobatake, S. Photochromism of diarylethene  
20 molecules and crystals: Memories, switches, and actuators. *Chem. Rev.* **2014**, *114*,  
21 12174–12277.  
22  
23  
24  
25 (12) Jayasuriya, N.; Kagan, J.; Owens, J. E.; Kornak, E. P.; Perrine, D. M. Photocyclization  
26 of terthiophenes. *J. Org. Chem.* **1989**, *54*, 4203–4205.  
27  
28  
29  
30 (13) Takeshita, M.; Hirowatari, T.; Takedomi, A. E/Z isomerization of a thermally bistable  
31 photochromic dithienylethene. *Tetrahedron Lett.* **2016**, *57*, 3565–3567.  
32  
33  
34  
35 (14) Wang, R.; Ding, H.; Pu, S.; Xia, H.; Liu, G. Syntheses, photochromism and polarization  
36 optical recording of a novel diarylethene having a thiazole unit. *International Congress*  
37 *on Image and Signal Processing* **2010**, 2849–2852.  
38  
39  
40  
41 (15) Ishibashi, Y.; Umesato, T.; Fujiwara, M.; Une, K.; Yoneda, Y.; Sotome, H.;  
42 Katayama, T.; Kobatake, S.; Asahi, T.; Irie, M.; Miyasaka, H. Solvent Polarity Depen-  
43 dence of Photochromic Reactions of a Diarylethene Derivative As Revealed by Steady-  
44 State and Transient Spectroscopies. *Phys. Chem. Chem. Phys.* **2016**, *120*, 1170–1177.  
45  
46  
47  
48 (16) Motoyama, K.; Li, H.; Koike, T.; Hatakeyama, M.; Yokojima, S.; Nakamura, S.;  
49 Akita, M. Photo- and electro-chromic organometallics with dithienylethene (DTE)  
50  
51  
52  
53  
54  
55  
56  
57  
58  
59  
60



- linker,  $L_2CpM-DTE-MCpL_2$ : Dually stimuli-responsive molecular switch. *Dalton Trans.* **2011**, *40*, 10643.
- (17) Liu, Y.; Lagrost, C.; Costuas, K.; Tchouar, N.; Le Bozec, H.; Rigaut, S. A multifunctional organometallic switch with carbon-rich ruthenium and diarylethene units. *Chem. Commun.* **2008**, *109*, 6117–6119.
- (18) Li, X.; Tian, H. One-step synthesis and photochromic properties of a stable triangle terthiophene. *Tetrahedron Lett.* **2005**, *46*, 5409–5412.
- (19) Li, X.; Ma, Y.; Wang, B.; Li, G. “Lock and key control” of photochromic reactivity by controlling the oxidation/reduction state. *Org. Lett.* **2008**, *10*, 3639–3642.
- (20) Kawai, T.; Iseda, T.; Irie, M. Photochromism of triangle terthiophene derivatives as molecular re-router. *Chem. Commun.* **2004**, 72–73.
- (21) Wang, J.; Gao, Y.; Zhang, J.; Tian, H. Invisible photochromism and optical anti-counterfeiting based on DA type inverse diarylethene. *J. Mater. Chem. C* **2017**, *5*, 4571–4577.
- (22) Erko, F. G.; Berthet, J.; Patra, A.; Guillot, R.; Nakatani, K.; Métivier, R.; Delbaere, S. Spectral , Conformational and Photochemical Analyses of Photochromic Revisited. *Eur. J. Org. Chem.* **2013**, 7809–7814.
- (23) Jukes, R. T. F.; Adamo, V.; Hartl, F.; Belser, P.; De Cola, L. Photochromic Dithienylethene Derivatives Containing Ru(II) or Os(II) Metal Units. Sensitized Photocyclization from a Triplet State. *Inorg. Chem.* **2004**, *43*, 2779–2792.
- (24) Fox, M. A.; Roberts, R. L.; Baines, T. E.; Le Guennic, B.; Halet, J.-F.; Hartl, F.; Yufit, D. S.; Albesa-Jové, D.; Howard, J. A. K.; Low, P. J. Ruthenium complexes of C,C'-bis(ethynyl)carboranes: An investigation of electronic interactions mediated by spherical pseudo-aromatic spacers. *J. Am. Chem. Soc.* **2008**, *130*, 3566–3578.

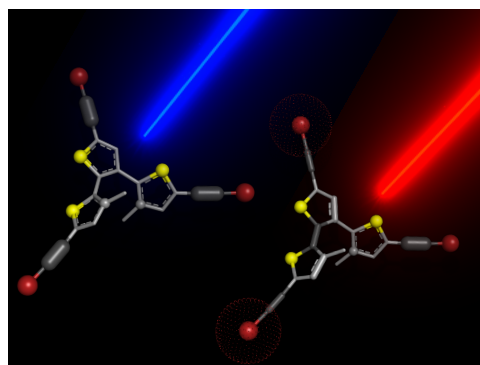
- 1  
2  
3 (25) Fitzgerald, E. C.; Ladjarafi, A.; Brown, N. J.; Collison, D.; Costuas, K.; Edge, R.;  
4 Halet, J.-F.; Justaud, F.; Low, P. J.; Meghezzi, H.; Roisnel, T.; Whiteley, M. W.;  
5 Lapinte, C. Spectroscopic Evidence for Redox Isomerism in the 1,4-Diethynylbenzene-  
6 Bridged Heterobimetallic Cation  $[\{\text{Fe}(\text{dppe})\text{Cp}^*\} (\mu\text{-C}\equiv\text{CC}_6\text{H}_4\text{C}\equiv\text{C})\{\text{Mo}(\text{dppe})(\eta\text{-}$   
7  $\text{C}_7\text{H}_7)\}\text{PF}_6$ . *Organometallics* **2011**, *30*, 4180–4195.  
8  
9  
10  
11  
12  
13  
14 (26) Bruce, M. I.; Costuas, K.; Davin, T.; Ellis, B. G.; Halet, J.-F.; Lapinte, C.; Low, P. J.;  
15 Smith, M. E.; Skelton, B. W.; Toupet, L.; White, A. H. Iron versus Ruthenium :  
16 Dramatic Changes in Electronic Structure Result from Replacement of One Fe by Ru  
17 in  $[\{\text{Cp}^*(\text{dppe})\text{Fe}\}\text{-CC-CC-}\{\text{Fe}(\text{dppe})\text{Cp}^*\}]^{n+}$  ( $n = 0, 1, 2$ ). *Organometallics* **2005**, *24*,  
18 3864–3881.  
19  
20  
21  
22  
23  
24  
25 (27) Steed, J.; Atwood, J. L. *Supramolecular Chemistry*; Wiley, Chichester, 2000.  
26  
27  
28 (28) Hervault, Y.-M.; Ndiaye, C. M.; Norel, L.; Lagrost, C.; Rigaut, S. Controlling the Step-  
29 wise Closing of Identical DTE Photochromic Units with Electrochemical and Optical  
30 Stimuli. *Org. Lett.* **2012**, *14*, 4454–4457.  
31  
32  
33  
34 (29) Zhang, J.; Sun, C.-F.; Zhang, M.-X.; Hartl, F.; Yin, J.; Yu, G.-A.; Rao, L.; Liu, S. H.  
35 Asymmetric oxidation of vinyl- and ethynyl terthiophene ligands in triruthenium com-  
36 plexes. *Dalton Trans.* **2016**, *45*, 768–782.  
37  
38  
39  
40  
41 (30) Peters, A.; McDonald, R.; Branda, N. R. Regulating  $\pi$ -conjugated pathways using a  
42 photochromic 1,2-dithienylcyclopentene. *Chem. Commun.* **2002**, 2274–2275.  
43  
44  
45  
46 (31) Woodward, R. B.; Hoffmann, R. H. *The Conservation of Orbital Symmetry*; Verlag  
47 Chemie, 1970.  
48  
49  
50  
51 (32) Lambert, C.; Moos, M.; Schmiedel, A.; Holzapfel, M.; Schäfer, J.; Kess, M.; Engel, V.  
52 How fast is optically induced electron transfer in organic mixed valence systems? *Phys.*  
53 *Chem. Chem. Phys.* **2016**, *18*, 19405–19411.  
54  
55  
56  
57  
58  
59  
60

- 1  
2  
3  
4 (33) Paa, W.; Yang, J.-P.; Helbig, M.; Hein, J.; Rentsch, S. Femtosecond time-resolved  
5 measurements of terthiophene: fast singlet-triplet intersystem crossing. *Chem. Phys.*  
6 *Lett.* **1998**, *292*, 607–614.  
7  
8  
9  
10 (34) Ishibashi, Y.; Mukaida, M.; Falkenström, M.; Miyasaka, H.; Kobatake, S.; Irie, M.  
11 One- and multi-photon cycloreversion reaction dynamics of diarylethene derivative with  
12 asymmetrical structure, as revealed by ultrafast laser spectroscopy. *Phys. Chem. Chem.*  
13 *Phys.* **2009**, *11*, 2640–2648.  
14  
15  
16  
17  
18 (35) Ishibashi, Y.; Umesato, T.; Kobatake, S.; Irie, M.; Miyasaka, H. Femtosecond Laser  
19 Photolysis Studies on Temperature Dependence of Cyclization and Cycloreversion Re-  
20 actions of a Photochromic Diarylethene Derivative. *J. Phys. Chem. C* **2012**, *116*, 4862–  
21 4869.  
22  
23  
24  
25  
26  
27 (36) Miyasaka, H.; Araki, S.; Tabata, A.; Nobuto, T.; Mataga, N.; Irie, M. Picosecond laser  
28 photolysis studies on photochromic reactions of 1,2-bis (2,4,5-trimethyl-3-thienyl)maleic  
29 anhydride in solutions. *Chem. Phys. Lett.* **1994**, *230*, 249–254.  
30  
31  
32  
33  
34 (37) Tamai, N.; Saika, T.; Shimidzu, T.; Irie, M. Femtosecond Dynamics of a Thiophene  
35 Oligomer with a Photoswitch by Transient Absorption Spectroscopy. *J. Phys. Chem.*  
36 **1996**, *100*, 4689–4692.  
37  
38  
39  
40  
41 (38) Okabe, C.; Nakabayashi, T.; Nishi, N.; Fukaminato, T.; Kawai, T.; Irie, M.; Sekiya, H.  
42 Picosecond Time-Resolved Stokes and Anti-Stokes Raman Studies on the Photochromic  
43 reactions of Diarylethene Derivatives. *J. Phys. Chem. A* **2003**, *107*, 5384–5390.  
44  
45  
46  
47 (39) Huerta-Viga, A.; Shaw, D. J.; Woutersen, S. pH Dependence of the Conformation of  
48 Small Peptides Investigated with Two-Dimensional Vibrational Spectroscopy. *J. Phys.*  
49 *Chem. B* **2010**, *114*, 15212–15220.  
50  
51  
52  
53  
54 (40) Limburg, B.; Hilbers, M.; Brouwer, A. M.; Bouwman, E.; Bonnet, S. The Effect of  
55 Liposomes on the Kinetics and Mechanism of the Photocatalytic Reduction of 5,5-  
56  
57  
58  
59  
60

- 1  
2  
3 Dithiobis(2-Nitrobenzoic Acid) by Triethanolamine. *J. Phys. Chem. B* **2016**, *120*,  
4 12850–12862.  
5  
6  
7  
8 (41) Frisch, M. J. et al. Gaussian09 Revision D.01. Gaussian Inc. Wallingford CT 2009.  
9  
10  
11 (42) Tachikawa, H.; Kawabata, H.; Ishida, K.; Matsushige, K. A DFT and direct MO dy-  
12 namics study on the structures and electronic states of phenyl-capped terthiophene. *J.*  
13 *Organomet. Chem.* **2005**, *690*, 2895–2904.  
14  
15  
16  
17 (43) Higashiguchi, K.; Matsuda, K.; Asano, Y.; Murakami, A.; Nakamura, S.; Irie, M. Pho-  
18 tochromism of Dithienylethenes Containing Fluorinated Thiophene Rings. *Eur. J. Org.*  
19 *Chem.* **2005**, 91–97.  
20  
21  
22  
23 (44) Al-Anber, M.; Milde, B.; Alhalasah, W.; Lang, H.; Holze, R. Electrochemical and DFT-  
24 studies of substituted thiophenes. *Electrochim. Acta* **2008**, *53*, 6038–6047.  
25  
26  
27  
28 (45) Gordon, K. C.; Clarke, T. M.; Officer, D. L.; Hall, S. B.; Collis, G. E.; Burrell, A. K.  
29 Vibrational spectra and calculations on substituted terthiophenes. *Synth. Met* **2003**,  
30 *137*, 1367–1368.  
31  
32  
33  
34 (46) Tomasi, J.; Mennucci, B.; Cammi, R. Quantum Mechanical Continuum Solvation Mod-  
35 els. *Chem. Rev.* **2005**, *105*, 2999–3094.  
36  
37  
38  
39 (47) Yanai, T.; Tew, D. P.; Handy, N. C. A new hybrid exchange-correlation functional  
40 using the Coulomb-attenuating method (CAM-B3LYP). *Chem. Phys. Lett.* **2004**, *393*,  
41 51–57.  
42  
43  
44  
45 (48) Hay, P. J.; Wadt, W. R. Ab initio effective core potentials for molecular calculations.  
46 Potentials for K to Au including the outermost core orbitals. *J. Chem. Phys.* **1985**, *82*,  
47 299–310.  
48  
49  
50  
51 (49) Snellenburg, J. J.; Laptanok, S. P.; Seger, R.; Mullen, K. M.; van Stokkum, I. H. M.  
52  
53  
54  
55  
56  
57  
58  
59  
60

- 1  
2  
3 Glotaran: a Java-based Graphical User Interface for the R-package TIMP. *J. Stat.*  
4 *Softw.* **2012**, *49*, 1–22.  
5  
6  
7  
8 (50) Henry, E. R. The use of matrix methods in the modeling of spectroscopic data sets.  
9 *Biophys. J.* **1997**, *72*, 652–73.  
10  
11  
12 (51) Scott, A. P.; Radom, L. Harmonic Vibrational Frequencies: An Evaluation of Hartree-  
13 Fock, Møller-Plesset, Quadratic Configuration Interaction, Density Functional Theory,  
14 and Semiempirical Scale Factors. *J. Phys. Chem.* **1996**, *100*, 16502–16513.  
15  
16  
17 (52) Gao, Y.; Liu, C.-G.; Jiang, Y.-S. Electronic Structure of Thiophene Oligomer Dications  
18 : An Alternative Interpretation from the Spin-Unrestricted DFT Study. *J. Phys. Chem.*  
19 *A* **2002**, *106*, 5380–5384.  
20  
21  
22 (53) Irle, S.; Lischka, H. An ab initio investigation of the charge-transfer complexes of alkali  
23 atoms with oligo ( $\alpha,\alpha'$ ) thiophenes and oligoparaphenylenes: A model calculation on  
24 polaronic and bipolaronic defect structures. *J. Chem. Phys.* **1995**, *103*, 1508–1522.  
25  
26  
27 (54) Irle, S.; Lischka, H. Combined ab initio and density functional study on polaron to  
28 bipolaron transitions in oligophenyls and oligothiophenes. *J. Chem. Phys.* **1997**, *107*,  
29 3021–3031.  
30  
31  
32  
33  
34  
35  
36  
37  
38  
39  
40  
41  
42  
43  
44  
45  
46  
47  
48  
49  
50  
51  
52  
53  
54  
55  
56  
57  
58  
59  
60

## For Table of Contents Only



Diarylethene is one of the most commonly used photoswitches in the molecular-electronics field. Interestingly, two new diarylethene-based compounds (incorporated into a non-C3-symmetric terthiophene core) show unexpectedly great resistance to photocyclisation. Time-resolved vibrational spectroscopy reveals that photo-switching is prevented by the asymmetric character of the excited state. These results provide a solid starting point for designing novel compounds in which asymmetry could be compatible with gating electron and energy transfer.